

# Microcomputed tomography–based structural analysis of various bone tissue regeneration models

Ilan Kallai<sup>1</sup>, Olga Mizrahi<sup>1</sup>, Wafa Tawackoli<sup>2</sup>, Zulma Gazit<sup>1,2</sup>, Gadi Pelled<sup>1,2</sup> & Dan Gazit<sup>1,2</sup>

<sup>1</sup>Skeletal Biotech Laboratory, The Hebrew University–Hadassah Faculty of Dental Medicine, Ein Kerem, Jerusalem, Israel. <sup>2</sup>Department of Surgery and Cedars-Sinai Regenerative Medicine Institute, Cedars-Sinai Medical Center, Los Angeles, California, USA. Correspondence should be addressed to D.G. (dgaz@cc.huji.ac.il).

Published online 6 January 2011; doi:10.1038/nprot.2010.180

**Microcomputed tomography (microCT) analysis is a powerful tool for the evaluation of bone tissue because it provides access to the 3D microarchitecture of the bone. It is invaluable for regenerative medicine as it provides the researcher with the opportunity to explore the skeletal system both *in vivo* and *ex vivo*. The quantitative assessment of macrostructural characteristics and microstructural features may improve our ability to estimate the quality of newly formed bone. We have developed a unique procedure for analyzing data from microCT scans to evaluate bone structure and repair. This protocol describes the procedures for microCT analysis of three main types of mouse bone regeneration models (ectopic administration of bone-forming mesenchymal stem cells, and administration of cells after both long bone defects and cranial segmental bone defects) that can be easily adapted for a variety of other models. Precise protocols are crucial because the system is extremely user sensitive and results can be easily biased if standardized methods are not applied. The suggested protocol takes 1.5–3.5 h per sample, depending on bone tissue sample size, the type of equipment used, variables of the scanning protocol and the operator's experience.**

## INTRODUCTION

Tissue engineering is a rapidly growing field designed to provide biological replacement therapies for damaged tissues and organs. Previously, we demonstrated success in the use of mesenchymal stem cells (MSCs), which are multipotent adult stem cells, for skeletal and bone tissue regeneration<sup>1</sup>.

Advanced microimaging methods have an increasingly important role in the rigorous evaluation of tissue regeneration strategies. Microcomputed tomography (MicroCT) is an X-ray–based imaging method that provides easy and relatively inexpensive access to the 3D microarchitecture of bone. This imaging modality is based on a microfocus X-ray source that illuminates the object and a planar detector that collects magnified projection images. Hundreds of angular views are acquired while the object of interest rotates. From these views, a computer synthesizes a stack of virtual cross-sections, interpolating sections along different planes, to inspect the internal structure of the object. On the basis of these data, the computer can reconstruct a realistic 3D image and cut it into slices to produce 2D images<sup>2</sup>. A quantitative 3D histomorphometric evaluation (i.e., determination of the volume of bone mass and of the microarchitecture indices of the newly formed bone) can then be performed on a cubic volume or on an irregularly shaped volume of interest (VOI). The VOI is defined by a set of freehand contours or by geometric objects such as rectangles or ellipses. The VOI must be drawn using a slice-based method.

MicroCT is an invaluable tool for skeletal regenerative medicine because it provides the researcher with the opportunity to explore the skeletal system both *in vivo* and *ex vivo*. The quantitative assessment of the bone's macrostructural characteristics, such as geometry, and its microstructural features, such as relative mineralized bone volume (BV), bone thickness and connectivity, may improve our ability to estimate the quality of regenerated bone.

Recent published protocols and studies describe different approaches to microCT scanning and analysis for several musculoskeletal applications, including (i) analysis of bone remodeling in a rat calvarial defect model<sup>3</sup> and (ii) long bone fracture healing<sup>4</sup>. These publications are, however, either not detailed enough that

researchers can successfully implement the protocol by themselves<sup>3</sup> or are based on a multithresholding separation of the newly formed callus from the native bone, which is specific to one type of microCT equipment and cannot be easily modified to suit other systems<sup>4</sup>.

In this paper, we provide a comprehensive protocol that covers the main types of bone regeneration models frequently used in the literature. Although the protocol was designed on the basis of the authors' experience using a specific microCT system, the procedures are described using general terminology, thus allowing this protocol to be applied to various microCT systems.

## Development of the protocol

We have published several studies featuring bone tissue regeneration models in which microCT analysis had a major role in the evaluation of results<sup>5–9</sup>. In developing our microCT analysis procedures, we tested three main models of bone tissue regeneration in a mouse model, the experimental designs for which have been described elsewhere (see references for each model). These three types are as follows:

1. *Ectopic bone formation model*—In this model, bone formation is induced in a location where it is not normally expected to occur by injecting bone-forming MSCs intramuscularly<sup>7–10</sup> and subcutaneously<sup>6,11</sup>.
2. *Segmental defect in a long bone model*—In this model, a fracture is created in a long bone by removing a fragment of the bone. We induce non-union fracture repair in a mouse radial defect<sup>5,6,9,10,12</sup>. The surgical procedure to remove the bone segment is followed by implantation of bone-forming MSCs, seeded on a collagen sponge, into the fracture site.
3. *Round critical-size bone defect model*—This model is used for mandibular<sup>8</sup> and calvarial defect regeneration<sup>13</sup>. This is achieved by a surgical procedure to expose the bone, followed by creating a round defect with a drill. Implanting bone-forming MSCs into the round defect site induces bone regeneration.

## PROTOCOL

Bone formation in the sites of regeneration was evaluated by microCT analyses. In addition to the visual assessment of structural images provided by this technology, morphometric indices can be determined on the basis of microtomographic data sets by using direct 3D morphometry<sup>14</sup>. To quantify bone regeneration and compare it among several samples, a standardized method must be used.

The principles of our protocol primarily focus on the standardization of the samples and the proper selection and adjustments of the VOI for quantitative analysis. These procedural steps have a great effect on the outcomes of the analysis. Precise protocols are crucial in this type of analysis, because the system is extremely user sensitive and results can be easily biased if standardized methods are not applied.

### MATERIALS

#### REAGENTS

##### Tissue samples

Bone tissue was regenerated in three different models as described above:

(i) in the ectopic model, tissue was regenerated in the mouse thigh muscle; (ii) in the long bone segmental defect model, a 2.5-mm long bone defect was created in the mouse radius; and (iii) in the round critical-size bone defect model, a 1-mm-diameter defect was created in mouse mandible. In all three models, bone regeneration was achieved by the implantation of bone-forming MSCs. The materials and experimental design are described in detail elsewhere<sup>5,8,9</sup>. The regenerated bone samples were scanned and analyzed using the equipment mentioned below.

This protocol is designed to evaluate bone regeneration as an outcome of a specific treatment. To analyze the effect of the treatment, the results should be compared with a set of nontreated control samples. In the defect models

(long bone and round segmental defects), we highly recommended scanning the defected bone immediately (not later than 1 d) after creating the defects to compare the bone regeneration with the initial state. In addition, to obtain statistically meaningful results, the number of samples per experimental group should be at least five. Power analysis can be used to calculate the minimum sample size required.

#### EQUIPMENT

This protocol was designed for use with a Desktop Cone-Beam MicroCT Scanner ( $\mu$ CT 40; Scanco Medical). The evaluation of 3D scanned data was handled by the software provided with the scanner: IPL (Image Processing Language), an advanced, script-based, 3D volume analysis tool. In this protocol, we describe evaluation procedures conducted with Scanco microCT software version 6.0. Adjustments will be needed if another company's software is used.

### PROCEDURE

#### MicroCT scanning of new bone formation in regeneration sites ● TIMING 30–60 min per sample

1| Scan the regenerated bone tissue sample using the microCT scanner. The bone tissue sample can be scanned *in vivo* (option A); *ex vivo*, after harvesting the organ in which the bone formed (option B); or after harvesting newly formed bone tissue without the host organ (option C). (Note: option C is relevant only for the ectopic bone formation model.) Scanning the sample *in vivo*, if possible, has several advantages but also raises some concerns. It allows longitudinal, and thus less variable, investigations of bone regeneration, along with a reduction in the number of animals used per study. However, it can result in several issues worth consideration: (i) lower image resolution, due to the equipment settings used; (ii) a large amount of ionizing radiation delivered during the scans, which can affect the study results; and (iii) movement artifacts, due to the animal's breathing.

**! CAUTION** Research protocols involving the use of animals should be reviewed by the investigator's institutional ethical review board to avoid any unnecessary discomfort or pain to the animals and to determine whether alternatives exist to animal research. All animal experiments should be performed in accordance with relevant guidelines and regulations of protocols approved by the investigator's institutional animal research review committee. Personnel should be trained in animal handling.

**▲ CRITICAL STEP** Ensure that all samples of your experiment are scanned with the same scanning protocol settings (X-ray energy, scanning medium, intensity, voxel size and image resolution) and in similar orientation. This is necessary to compare data sets of the experimental design. Bouxsein *et al.*<sup>15</sup> elaborated the key steps and considerations involved in setting up microCT scanning for the assessment of bone microstructure in animal models.

#### ? TROUBLESHOOTING

#### Measurement of the angle for rotation and reconstruction of the 2D images ● TIMING 15–30 min per sample

2| Check the reconstructed 2D images of your sample. Ensure that all parts of your sample are scanned properly. If the sample was not aligned during scanning and a rotation is needed, measure the angle for rotation and reconstruct the 2D images again using the corrected rotation angle. (The IPL command lines for this rotation are provided in the **Supplementary Method**.)

#### Definition and adjustment of the VOI for the quantitative evaluation

3| This process depends on which bone formation model is used. Use option A for the ectopic bone formation model, option B for modeling a segmental defect in a long bone and option C for modeling round critical-size bone defects. (Detailed IPL command lines for options B and C are provided as a **Supplementary Method**.)

##### (A) Ectopic bone formation model ● TIMING 30–60 min

(i) Draw the VOI by contouring the boundaries of the ectopic bone tissue, as demonstrated in **Figure 1**. Ensure that all slices showing ectopic bone are processed.

#### ? TROUBLESHOOTING

##### (B) Segmental defect in a long bone model (radial non-union fracture repair) ● TIMING 60–90 min

(i) Check whether the sample is placed at a straight angle and aligned with the x axis, as shown in **Figure 2**. If not, the angle of the object must be changed (as noted in Step 2).

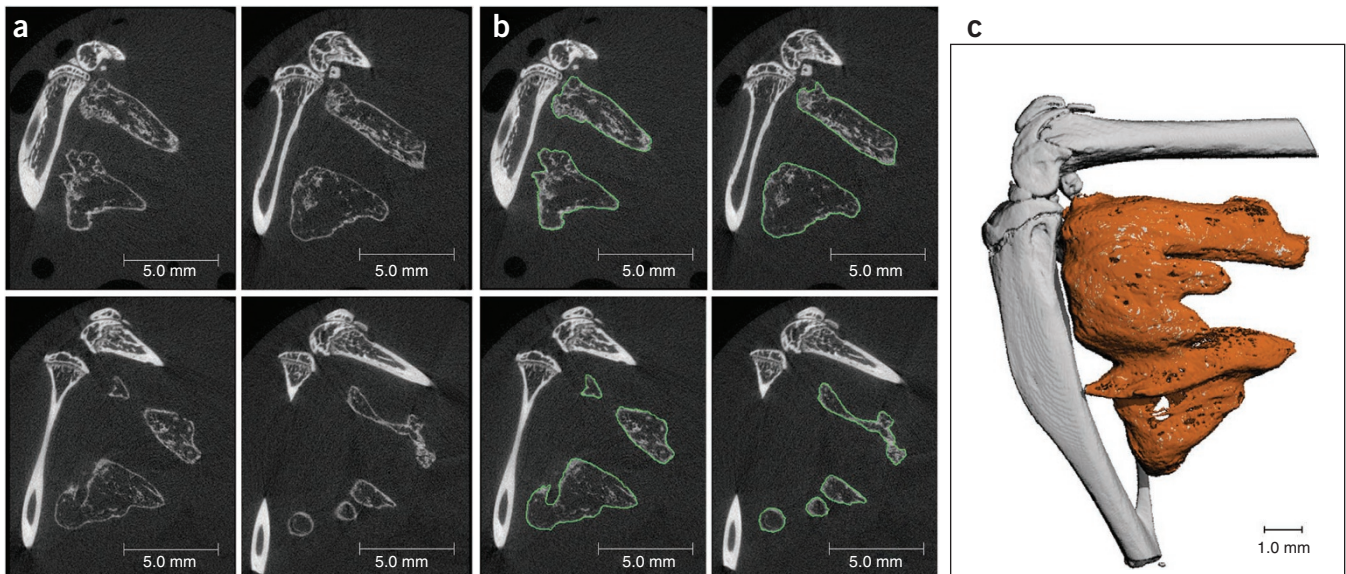


**Figure 1** | Ectopic bone formation model. (a) 2D slices of the sample, showing bone formation adjacent to native bones. (b) Contours of ectopic bone tissue, shown in green. (c) 3D image of the sample after 3D evaluation. The orange region shows the area of bone formation that was evaluated.

- (ii) The sample must be flipped. Its direction must be changed from the *xy* plane to the *zy* plane, as depicted in **Figure 2b**. To flip the sample axes, create a 3D object of the sample, rotate the object by 90°, and then slice the object again into 2D slices.
- (iii) Locate the margins of the defect by identifying the edges of native radial bone stumps. Select the range of slices for contouring so that it is located in the middle of the original defect site. This range must be a standard size for all samples.
- (iv) Contour the newly formed bone in the selected slice range without including native ulnar bone, as demonstrated in **Figure 2c**.

**? TROUBLESHOOTING**

**(C) Round critical-size bone defect model (mandible defect regeneration) ● TIMING 45–60 min**

- (i) A simple way to locate the margins of the defect is to create a 3D-segmented object of the sample (**Fig. 3**). Set the low-threshold value as high as possible to discard most of the newly formed bone in the defect site, as demonstrated in **Figure 3a**.
- (ii) Align the margins of the defect with the *x* and *y* axes. To determine the angles for turning, open the 3D-segmented file in the 3D preview program. Locate the middle of the defect in the 3D-segmented object along the *x* axis (**Fig. 3b**) and measure the angle of the defect margins (**Fig. 3c**). Turn the object according to the measured angle (with the ‘turn3D’ command in IPL). Open the turned-*x* 3D object (**Fig. 3d**) and repeat the previous step for the *y* axis (**Fig. 3e–g**). Open the turned-*xy* 3D object and ensure that the margins of the defect are now aligned. Turn the non-segmented 3D file of the sample using the same angles.

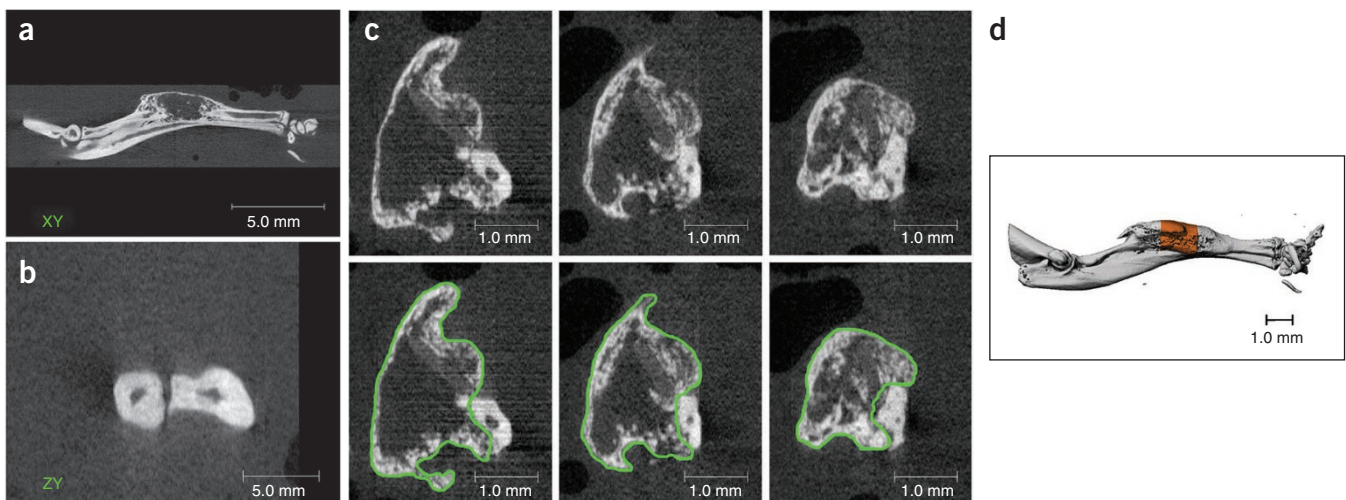
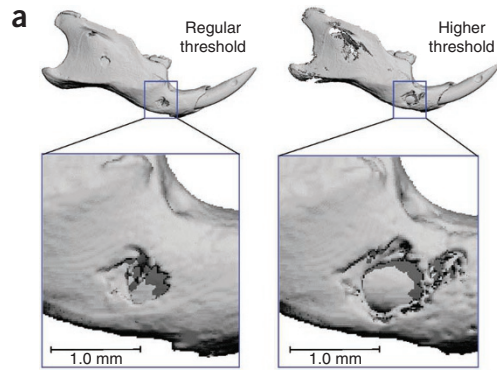


**Figure 2** | Segmental defect in a long bone model. (a) 2D slice showing the sample aligned with the *x* axis. (b) 2D slice after flipping the axes from the *xy* plane to the *zy* plane. (c) Contours of bone formation in the range of selected slices, not including the native ulnar bone. (d) 3D image of the sample after 3D evaluation. The evaluated bone formation in the defect site is shown in orange.

## PROTOCOL

**Figure 3** | Round critical-size bone defect model.

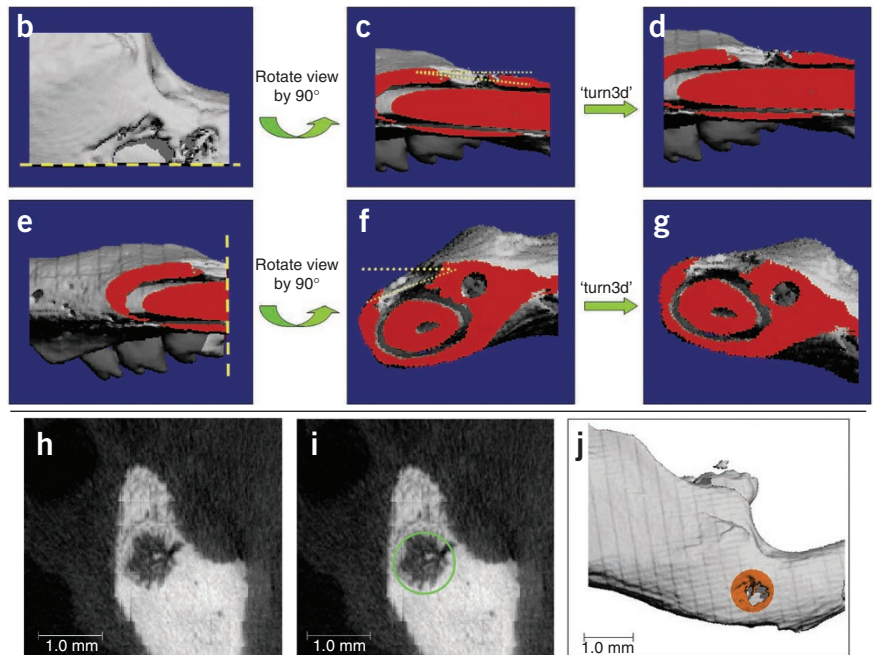
(a) 3D-segmented objects of the sample, with regular and high values for the lower threshold. (b) Locating the middle of the defect in the 3D-segmented object along the x axis. (c) Measurement of the angle of the defect margins. (d) 3D-segmented object after rotation of the x axis. (e–g) Repeating the procedure shown in b–d for the y axis. (h) 2D slice of the xy-turned non-segmented object, showing the defect. (i) Round object contour defines the VOI for 3D evaluation. (j) 3D image of the sample after the 3D evaluation. The evaluated bone formation in the defect site is shown in orange.



(iii) Again, slice the turned-xy non-segmented object into 2D slices. Locate the defect region in the 2D slices (**Fig. 3h**).

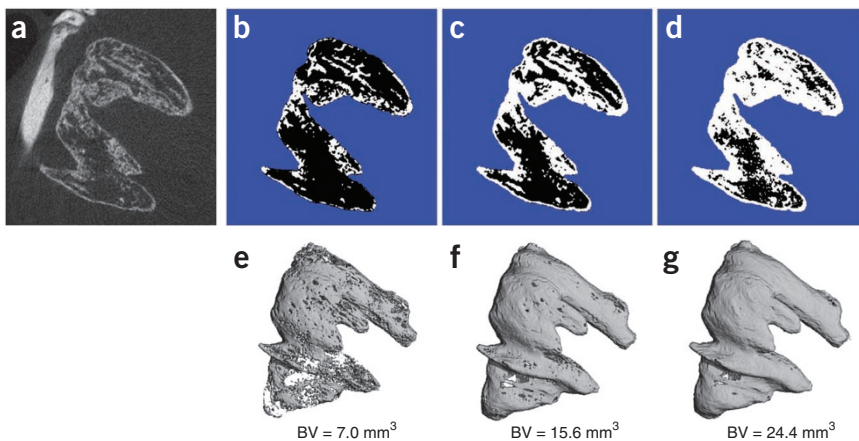
### ? TROUBLESHOOTING

(iv) Define the VOI by using a round object contour. To create a cylindrical shape that will pass through the defect area, choose the ellipse shape and determine its size (usually this should be the size of the defect created). Situate the round contour at the center of the defect on all relevant slices (**Fig. 3i**). For a better comparison between samples, ensure that the number of slices is identical in each sample. This will allow you to compare the percentage of healing between samples (evaluated by the BV to total volume (TV) ratio (BV/TV)).



### 3D histomorphometric evaluation ● TIMING 5–30 min per sample

4| Set the values for the 3D histomorphometric evaluation. Use a constrained 3D Gaussian filter to partly suppress the noise in the volumes (common values: standard deviation ( $\sigma$ ) = 0.8, support = 1). When performing a 3D evaluation of an object, you must set a threshold (see **Fig. 4**). From the grayscale image, you can create a binary image (segmented) by thresholding. All voxels below the lower-threshold set and above the upper-threshold set will be set to value 0; the remaining voxels (the object) will be given a value in range.



▲ **CRITICAL STEP** When you determine the threshold you must pay attention to the following key points (see **Fig. 4**):

**Figure 4** | Setting the lower threshold. (a) Grayscale, unsegmented image of ectopic bone formation. (b) Threshold is set too high, resulting in disappearance and thinning of the bone structures. (c) Threshold is set correctly, showing reasonable binarization of bone structures. (d) Threshold is set too low, resulting in thickening of the bone structures and appearance of 'noise' in the object. (e–g) 3D images of bone formation after 3D evaluation. The bone volume (BV) of bone formation is shown in order to demonstrate the effect of threshold-setting on quantitative results.

(i) The lower threshold should be high enough to avoid thickening of the bone structures and appearance of ‘noise’ in the object, as depicted in **Figure 4d**; (ii) The lower threshold should be low enough to avoid massive bone loss, i.e., disappearance or thinning of the bone structures, as depicted in **Figure 4b**; (iii) The upper threshold is usually set to the maximum value; (iv) Once you set the values, use the same values for all samples in the study.

**? TROUBLESHOOTING**

5| Send the VOI for evaluation with one of the scripts available in the evaluation program. (A detailed evaluation script is provided as a **Supplementary Method**.)

6| Save the qualitative results as 3D images and 2D cross-sections.

**? TROUBLESHOOTING**

Troubleshooting advice can be found in **Table 1**.

**TABLE 1** | Troubleshooting table.

Step	Problem	Solution
1	Image is not adequate for image analysis (noisy, scattered, low resolution, etc.)	Adjust the variables of the scanning protocol to better suit the sample’s characteristics. Guidelines for scanning protocol setting are described by Buxsein <i>et al.</i> <sup>15</sup>
3A(i) and 3B(iv)	Boundaries of the bone are not clear for contouring	Apply the same contour shape used in adjacent slices Do not apply a precise contour of the boundaries. Make sure that all required bone structures are included within the contour. Keep in mind that using non-precise contouring will lead to different results; therefore, same contouring method must be applied in all samples that are being compared
3C(iii)	The defect location in the 2D slices is not clear	Create another 3D-segmented object of the sample. Set the lower threshold value as high as possible in order to discard most of the newly formed bone in the defect site. Locate the defect in the 3D object and get the coordinates (x, y and z) of the defect center
4	The required lower threshold causes appearance of too much ‘noise’ in the object	Set the Gaussian filter with higher values to suppress the noise in the object

**● TIMING**

The required time to complete each of the steps detailed in this protocol depends on bone tissue sample size, type of equipment used (scanner, computer and software), variables of the scanning protocol and operator’s experience. Therefore, only a general estimation of the time frame needed is indicated.

Step 1, MicroCT scanning of the regenerated bone tissue samples: 30–60 min per sample

Step 2, Measurement of the angle for rotation and reconstruction of the 2D images with the corrected rotation angle: 15–30 min per sample

Step 3A, VOI definition and adjustment in the ectopic bone formation model: 30–60 min per sample

Step 3B, VOI definition and adjustment in the segmental defect–long bone model: 60–90 min per sample

Step 3C, VOI definition and adjustment in the round critical-size bone defect model: 45–60 min per sample

Steps 4–6, 3D histomorphometric evaluation: 5–30 min per sample

**ANTICIPATED RESULTS**

Evaluation of the regenerated bone tissue should be carried out by (i) qualitative assessment of the bone structure based on 2D cross-sections and 3D images, as illustrated in the figures for each model (**Figs. 1c, 2d and 3j**); and (ii) quantitative assessment of the bone structure on the basis of microtomographic data sets generated by direct 3D morphometry.

The following morphometric indices can be determined for newly formed bone in regeneration sites: (i) TV of bone, including new bone and soft-tissue cavities (TV, mm<sup>3</sup>); (ii) volume of mineralized bone tissue (BV, mm<sup>3</sup>); (iii) bone volume density, which can also be referred to as the percentage of regeneration for the round critical-size bone defect model (BV/TV, a ratio and hence no unit of measure); (iv) connectivity density (Conn.Dens., 1 per mm<sup>3</sup>), which is derived from the Euler number<sup>16</sup>

**TABLE 2** | Morphometric indices corresponding to the specific samples shown in **Figures 1–4**.

	TV (mm <sup>3</sup> )	BV (mm <sup>3</sup> )	BV/TV	Conn.Dens. (1 per mm <sup>3</sup> )	B.Th (mm)	B.Sp (mm)	BMD (mg HA per cm <sup>3</sup> )	DA
Ectopic bone formation	7.13	1.59	0.22	50.48	0.09	0.89	599.21	1.59
Radial non-union fracture repair	6.35	2.35	0.37	58.88	0.12	0.48	812.20	1.37
Mandible defect regeneration	0.33	0.13	0.38	6.03	0.16	0.26	994.33	1.61

and is a topological measure used to describe the porosity of the bone sample and to show how branched the bone tissue structure is; (v) average bone thickness (B.Th, mm), calculated as the average thickness of all bone voxels and abbreviated as 'Tb.Th\*' by Hildebrand *et al.*<sup>14</sup>; (vi) average bone separation, which is the thickness of cavities (B.Sp, mm) and abbreviated as 'Tb.Sp\*' by Hildebrand *et al.*<sup>14</sup>; (vii) bone mineral density (BMD, mg hydroxyapatite per cm<sup>3</sup>), derived from comparison of X-ray attenuation in the scanned bone sample with that of hydroxyapatite standards; and (viii) degree of anisotropy (DA).

**Table 2** presents the morphometric indices determined for the specific samples shown in this protocol (one sample per model).

*Note: Supplementary information is available in the HTML version of this article.*

**ACKNOWLEDGMENTS** We acknowledge funding from the National Institutes of Health grant nos. R01AR056694 and R01DE019902 and from the Telemedicine and Advanced Technology Research Center (TATRC), U.S. Army Medical Research and Materiel Command No. 08217008 (W.T., Z.G., G.P. and D.G.).

**AUTHOR CONTRIBUTIONS** I.K. developed the concept, designed the protocol and contributed to writing the manuscript. O.M. provided helpful comments during the development of the protocol and contributed to writing the manuscript. W.T. provided technical support and conceptual advice. G.P. provided helpful comments and contributed to writing the manuscript. Z.G. and D.G. supervised the project. All authors discussed the implications of the protocol and commented on the manuscript at all stages.

**COMPETING FINANCIAL INTERESTS** The authors declare no competing financial interests.

Published online at <http://www.natureprotocols.com/>.

Reprints and permissions information is available online at <http://npg.nature.com/reprintsandpermissions/>.

- Kimelman, N., Pelled, G., Gazit, Z. & Gazit, D. Applications of gene therapy and adult stem cells in bone bioengineering. *Regen. Med.* **1**, 549–561 (2006).
- Holdsworth, D.W. & Thornton, M.M. Micro-CT in small animal and specimen imaging. *Trends Biotechnol.* **20**, S34–S39 (2002).
- Umoh, J.U. *et al.* *In vivo* micro-CT analysis of bone remodeling in a rat calvarial defect model. *Phys. Med. Biol.* **54**, 2147–2161 (2009).
- Yeung, H. *et al.* Protocols of micro-computed tomographic analysis established for musculoskeletal applications. In *A Practical Manual for Musculoskeletal Research* (eds. Leung, K., Qin, L. & Cheung, W.) 279–300 (World Scientific Publishing, Singapore, 2008).

- Kallai, I. *et al.* Quantitative, structural, and image-based mechanical analysis of nonunion fracture repaired by genetically engineered mesenchymal stem cells. *J. Biomech.* **43**, 2315–2320 (2010).
- Kimelman-Bleich, N. *et al.* The use of a synthetic oxygen carrier-enriched hydrogel to enhance mesenchymal stem cell-based bone formation *in vivo*. *Biomaterials* **30**, 4639–4648 (2009).
- Pelled, G. *et al.* Structural and nanoindentation studies of stem cell-based tissue-engineered bone. *J. Biomech.* **40**, 399–411 (2007).
- Steinhardt, Y. *et al.* Maxillofacial-derived stem cells regenerate critical mandibular bone defect. *Tissue Eng. Part A* **14**, 1763–1773 (2008).
- Zilberman, Y. *et al.* Fluorescence molecular tomography enables *in vivo* visualization and quantification of nonunion fracture repair induced by genetically engineered mesenchymal stem cells. *J. Orthop. Res.* **26**, 522–530 (2008).
- Moutsatsos, I.K. *et al.* Exogenously regulated stem cell-mediated gene therapy for bone regeneration. *Mol. Ther.* **3**, 449–461 (2001).
- Turgeman, G. *et al.* Engineered human mesenchymal stem cells: a novel platform for skeletal cell mediated gene therapy. *J. Gene Med.* **3**, 240–251 (2001).
- Tai, K. *et al.* Nanobiomechanics of repair bone regenerated by genetically modified mesenchymal stem cells. *Tissue Eng. Part A* **14**, 1709–1720 (2008).
- Gafni, Y. *et al.* Gene therapy platform for bone regeneration using an exogenously regulated, AAV-2-based gene expression system. *Mol. Ther.* **9**, 587–595 (2004).
- Hildebrand, T., Laib, A., Muller, R., Dequeker, J. & Rueggsegger, P. Direct three-dimensional morphometric analysis of human cancellous bone: microstructural data from spine, femur, iliac crest, and calcaneus. *J. Bone Miner. Res.* **14**, 1167–1174 (1999).
- Bouxsein, M.L. *et al.* Guidelines for assessment of bone microstructure in rodents using micro-computed tomography. *J. Bone Miner. Res.* **25**, 1468–1486 (2010).
- Odgaard, A. & Gundersen, H.J. Quantification of connectivity in cancellous bone, with special emphasis on 3-D reconstructions. *Bone* **14**, 173–182 (1993).

